Materials Transactions, Vol. 49, No. 6 (2008) pp. 1474 to 1479

EXPRESS REGULAR ARTICLE

Phase Equilibria and Microstructure on γ' Phase in Co-Ni-Al-W System

Kazuya Shinagawa[1,*1], Toshihiro Omori[1], Jun Sato[1,*2], Katsunari Oikawa[1], Ikuo Ohnuma[1], Ryosuke Kainuma[2] and Kiyohito Ishida[1]

[1]*Department of Materials Science, Graduate School of Engineering, Tohoku University, Sendai 980-8579, Japan*
[2]*Institute of Multidisciplinary Research for Advanced Materials, Tohoku University, Sendai 980-8577, Japan*

Phase equilibria between the γ and γ' phases at 900°C in the Co-(10–70)Ni-Al-W system were determined by electron probe microanalysis (EPMA) and X-ray diffractometry (XRD). It was found that the γ' phase with $L1_2$ structure continuously exists from the Co side to the Ni side in Co-Ni-Al-W system and that it widens to the low W region with increasing Ni content. The partition of Al into the γ' phase increased with Ni content, while the W changed from a γ' former to a γ former by increase of Ni content. Differential scanning calorimetry (DSC) measurements also revealed that the γ' solvus temperature increases with Ni content, while the solidus temperature is hardly affected by such content. The lattice parameter of the γ and γ' phases and the mismatch decreased with increasing Ni content, which caused the morphologic change of the γ' precipitates from cubes to spheres. [doi:10.2320/matertrans.MER2008073]

(Received February 27, 2008; Accepted April 1, 2008; Published May 25, 2008)

Keywords: *cobalt-nickel-aluminum-tungsten, phase equilibria, phase stability, $L1_2$ compound, lattice parameter, superalloy*

1. Introduction

The Ni-based superalloys strengthened by precipitation of the γ' (Ni_3Al) phase with the $L1_2$ structure in the γ matrix (A1) have been widely utilized for high-temperature applications including aircraft engines and power generation systems, where the γ' phase shows positive temperature dependence of the strength. On the other hand, the GCP (geometrically close-packed) phase has not been successfully utilized in Co-based superalloys. In Co-based binary systems, only the Co_3Ti phase is known to be a stable $L1_2$ compound and the effects of alloying elements on the stability and morphology of the Co_3Ti γ' phase have been investigated. However, the microstructural stability is low due to the large mismatch in lattice constant between the γ and γ' phases in the binary system and application of the γ' phase is restricted to temperatures below 800°C due to the low phase stability of Co-Ti-based alloys containing alloying elements.[1)] On the other hand, the metastable γ' phase in several binary systems, such as Co-Ta,[2–4)] Co-Al[5–7)] and Co-W[8,9)] systems, has been reported, but its stability is too low for high temperature applications. Therefore, conventional Co-based superalloys have been strengthened by solid-solution hardening and carbide precipitation hardening, although the high-temperature strength is inferior to that of Ni-based superalloys.

We have recently found a new stable γ' phase with the $L1_2$ structure represented by the formula $Co_3(Al,W)$ in the Co-Al-W alloys,[10)] where the cuboidal γ' precipitates align along ⟨001⟩ of the γ matrix or spherical γ' precipitates in the γ matrix, which is similar to the morphology of the Ni-based superalloys. More recently, it has been reported that the polycrystalline and single-crystal Co-Al-W-based alloys exhibit anomalous temperature dependence of flow stress[11–13)] and that the high temperature strength of Co-Al-W-Ta alloy is comparable to that of the Ni-based superalloy MarM247 above 900°C.[13)]

It is expected that the phase stability of the γ' greatly increases by Ni substitution for Co because the Ni_3Al with the $L1_2$ structure is very stable and the γ' phase exists in a wide composition range in the Ni-Co-Al ternary phase diagram.[14)] A detailed phase diagram of Co-Ni-Al-W system is thus important for the design of not only Co-based but also Ni-based superalloys. In this study, the phase equilibria focusing on the relation between the γ and γ' phases in the Co-Ni-Al-W system were investigated and the morphology of the γ' precipitates is herein discussed in terms of the lattice mismatch.

2. Experimental Procedures

Co-(0–80)at%Ni-(5.6–20)at%Al-(2.5–10)at%W alloys were prepared from Co (99.9%), Ni (99.99%), Al (99.7%) and W (99.9%) by induction melting under an argon atmosphere. Small pieces of specimens were cut from the ingots and heat-treated at 1300°C for 24 hours, followed by quenching in ice water. The specimens were then heat-treated at 900°C for 168 hours, the specimens for composition analysis being cold-rolled at a reduction rate of 20–50% before the treatment at 900°C.

The equilibrium compositions of the γ and γ' phases at 900°C were determined by electron probe microanalysis (EPMA), and the phase transition temperatures were examined by differential scanning calorimetry (DSC) at a heating rate of 10°C/min.

X-ray diffraction (XRD) with Cu-Kα was carried out at room temperature to determine the lattice parameter of the γ and γ' phases, the Nelson-Riley function[15)] being used. The microstructure was observed using a field-emission scanning electron microscope (FE-SEM).

3. Results and Discussion

3.1 Phase equilibria

Figure 1 shows backscattered electron images of (a) Co-10Ni-10Al-7.5W and (b) Co-70Ni-10Al-7.5W alloys cold-rolled at a reduction rate of 50% and heat-treated at 900°C

*1Graduate Student, Tohoku University
*2Graduate Student, Tohoku University. Present Address: Hitachi Research Laboratory, Hitachi Ltd., Hitachi 319-1292, Japan

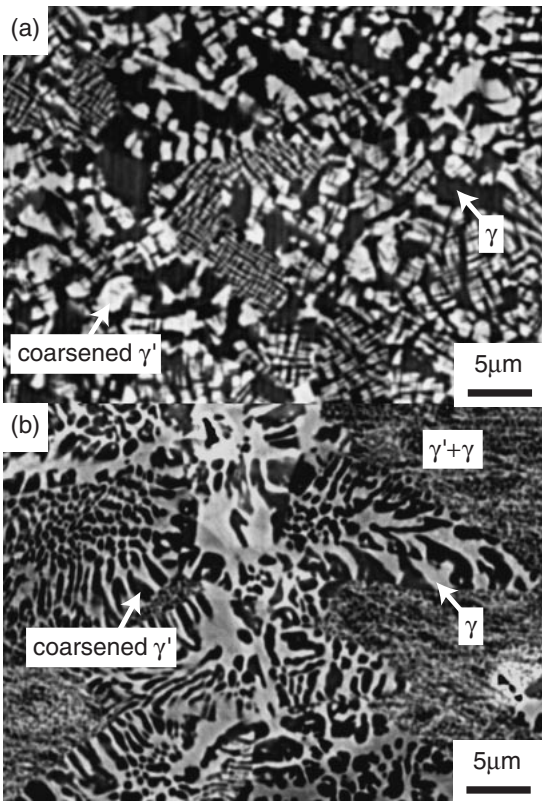

Fig. 1 Backscattered electron micrographs of (a) Co-10Ni-10Al-7.5W and (b) Co-70Ni-10Al-7.5W alloys cold-rolled at a reduction rate of 50% and annealed at 900°C for 168 hours.

for 168 hours. Since the coherent γ' precipitates are usually fine in the case of simple annealing, the cold-rolling was conducted in advance of the heat-treatment at 900°C to promote diffusion and to coarsen the γ/γ' microstructure sufficiently to determine the equilibrium compositions using EPMA. As shown in Fig. 1, some regions show relatively fine γ/γ' two-phase microstructure, while the size of each phase in some regions is larger than 1 μm, and thus available for quantitative analysis. From composition analysis, the dark and white phases in Fig. 1(a) are the γ and γ' phases, respectively, while the contrast is reversed in Fig. 1(b), which is caused by the change of the partition of Al and W into the γ and γ' phases as described later.

All the data obtained by the analysis for the Co-(10–70)at%Ni-Al-W alloys are listed in Table 1, where the $D0_{19}$ (Co_3W), B2 (CoAl), $D8_5$ (Co_7W_6) and A2 (W) phases are designated as χ, β, μ and α, respectively. The μ and α phases in the Co-60Ni-10Al-10W and Co-70Ni-10Al-10W alloys precipitated together and were too fine to determine the composition of each phase using EPMA. The β phase in Co-10Ni-12.5Al-7.5W alloy was also too fine due to the small amount of the precipitates. It can be seen that the γ' phase exists in all the specimens at 900°C and that the equilibrium compositions of Ni in the γ and γ' phases are not so different between phases. Therefore, the phase constitutions of Co-10Ni-Al-W, Co-30Ni-Al-W, Co-50Ni-Al-W and Co-70Ni-Al-W alloys are given in (Co+Ni)-Al-W two-dimensional figures as shown in Fig. 2, assuming that the Ni contents are equal in the γ and γ' phases and also in the χ, β, μ and α

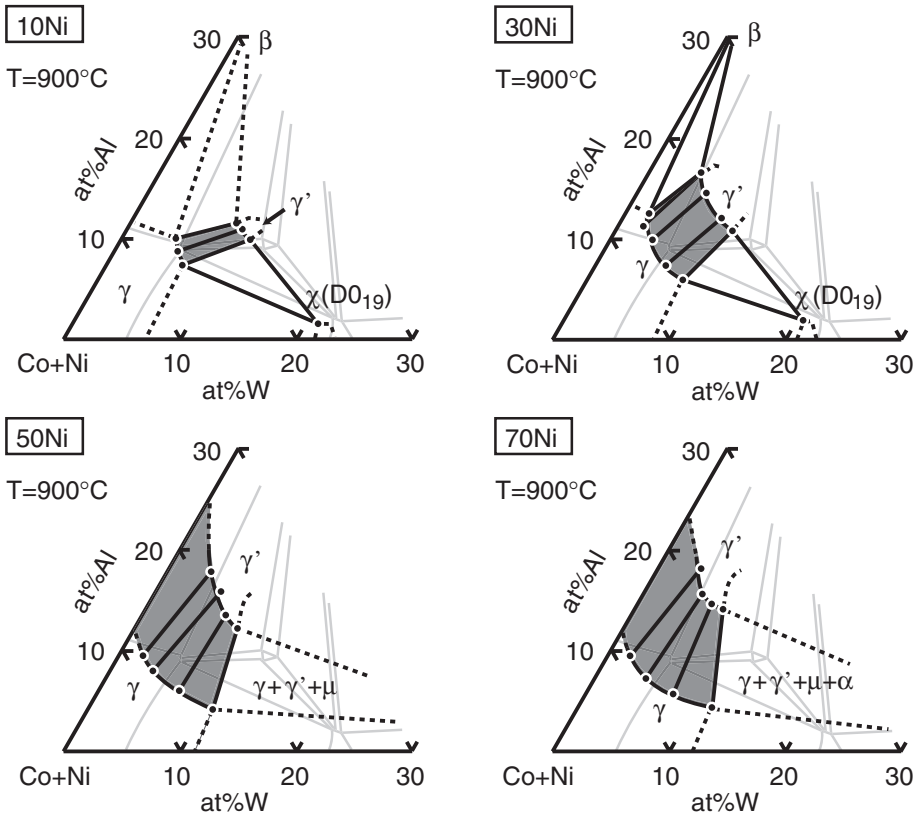

Fig. 2 Isothermal section diagram of Co-10Ni-Al-W, Co-30Ni-Al-W, Co-50Ni-Al-W and Co-70Ni-Al-W systems at 900°C. Grey lines and shaded regions indicate the phase boundaries in Co-Al-W ternary system[10] and the γ/γ' two-phase regions in Co-Ni-Al-W quaternary system, respectively.

Table 1 Equilibrium compositions of Co-(10–70)Ni-Al-W system at 900°C, where the A1, $L1_2$, $D0_{19}$ (Co_3W), B2 (CoAl), $D8_5$ (Co_7W_6) and A2 (W) phases are designated as γ, γ', χ, β, μ and α, respectively.

Composition of Specimen (at%)			γ (A1) (at%)			γ' ($L1_2$) (at%)			χ ($D0_{19}$) (at%)			μ ($D8_5$) (at%)			β (B2) (at%)		
Ni	Al	W	Ni	Al	W	Ni	Al	W	Ni	Al	W	Ni	Al	W	Ni	Al	W
10.0	10.0	10.0	11.2	7.3	6.3	10.7	9.8	11.1	6.6	1.5	20.9	—	—	—	—	—	—
10.0	10.0	7.5	9.7	8.7	5.4	10.5	10.8	9.9	—	—	—	—	—	—	—	—	—
10.0	12.5	7.5	9.2	10.0	4.7	10.3	11.5	9.1	—	—	—	—	—	—	nd	nd	nd
20.0	10.0	10.0	19.4	7.4	7.9	20.7	9.9	10.1	13.2	3.1	18.8	—	—	—	—	—	—
20.0	10.0	7.5	18.7	7.9	5.5	20.9	11.1	8.6	—	—	—	—	—	—	—	—	—
20.0	12.5	5.0	18.3	11.0	3.3	21.7	14.0	6.8	—	—	—	—	—	—	—	—	—
20.0	15.0	5.0	17.9	11.5	3.2	21.4	14.3	6.9	—	—	—	—	—	—	26.2	33.6	0.6
30.0	10.0	10.0	27.5	5.9	8.2	31.7	10.8	10.0	17.5	1.8	20.6	—	—	—	—	—	—
30.0	10.0	7.5	27.7	7.3	6.0	32.6	12.1	8.4	—	—	—	—	—	—	—	—	—
30.0	12.5	5.0	27.2	9.9	3.5	33.0	14.6	6.4	—	—	—	—	—	—	—	—	—
30.0	12.5	2.5	29.3	11.3	2.0	37.0	16.6	4.5	—	—	—	—	—	—	—	—	—
30.0	17.5	2.5	26.4	12.5	1.9	33.8	16.8	4.3	—	—	—	—	—	—	34.9	32.9	0.2
40.0	10.0	10.0	35.9	4.6	9.6	41.1	10.9	9.5	24.0	1.8	20.0	—	—	—	—	—	—
40.0	10.0	7.5	36.7	6.3	6.6	42.3	12.6	7.7	—	—	—	—	—	—	—	—	—
40.0	12.5	5.0	35.6	8.7	3.5	43.3	15.1	5.8	—	—	—	—	—	—	—	—	—
40.0	12.5	2.5	37.6	10.6	1.8	47.1	17.6	4.0	—	—	—	—	—	—	—	—	—
40.0	20.0	2.5	32.6	13.7	1.0	41.6	18.7	2.9	—	—	—	—	—	—	39.7	32.5	0.1
50.0	10.0	10.0	46.9	4.1	10.7	52.9	12.2	8.8	—	—	—	25.5	2.1	37.9	—	—	—
50.0	10.0	7.5	46.5	6.0	6.9	52.8	13.6	7.1	—	—	—	—	—	—	—	—	—
50.0	12.5	5.0	46.5	8.0	3.6	54.2	15.9	5.5	—	—	—	—	—	—	—	—	—
50.0	12.5	2.5	47.4	9.5	1.8	56.0	17.8	3.7	—	—	—	—	—	—	—	—	—
60.0	10.0	10.0	57.6	4.1	11.4	62.0	13.2	8.2	—	—	—	*	*	*	—	—	—
60.0	10.0	7.5	57.7	5.3	7.6	61.7	14.2	7.0	—	—	—	—	—	—	—	—	—
60.0	12.5	5.0	56.8	7.4	4.0	62.1	16.2	5.3	—	—	—	—	—	—	—	—	—
60.0	12.5	2.5	57.3	9.3	1.7	63.0	18.1	3.5	—	—	—	—	—	—	—	—	—
70.0	10.0	10.0	70.6	4.3	11.5	70.3	14.2	7.6	—	—	—	*	*	*	—	—	—
70.0	10.0	7.5	70.3	5.6	7.6	69.6	14.6	6.3	—	—	—	—	—	—	—	—	—
70.0	12.5	5.0	70.2	7.2	4.3	70.1	15.6	5.0	—	—	—	—	—	—	—	—	—
70.0	12.5	2.5	69.5	9.4	1.8	69.8	18.2	3.6	—	—	—	—	—	—	—	—	—

nd: not determined
*$\mu + \alpha$?

Table 2 Partition coefficient $K_x^{\gamma'/\gamma}$ $(= C_x^{\gamma'}/C_x^{\gamma})$ of each element in Co-xNi-10Al-7.5W at 900°C.

Specimen	Partition Coefficient $K_X^{\gamma'/\gamma} = C_X^{\gamma'}/C_X^{\gamma}$			
Co-xNi-10Al-7.5W	Co	Ni	Al	W
10Ni	0.90	1.08	1.24	1.86
20Ni	0.88	1.12	1.41	1.56
30Ni	0.79	1.18	1.66	1.41
40Ni	0.74	1.15	1.99	1.17
50Ni	0.65	1.13	2.26	1.03
60Ni	0.58	1.07	2.65	0.92
70Ni	0.57	0.99	2.63	0.84

phases for the sake of simplicity. The grey lines and shaded regions indicate the phase boundaries in Co-Al-W ternary system[10] and the γ/γ' two-phase region in Co-Ni-Al-W quaternary system, respectively. While the composition range of the stable γ' is small in the Co-Al-W ternary system, the γ' phase expands and shifts to lower W and higher Al content regions with increasing Ni content. Moreover, the γ' phase exists even without W in the composition region over 50% Ni, which can be confirmed by the Ni-Co-Al ternary phase diagram,[14] although the W is necessary to form the γ'–$L1_2$ compound in the region less than 40% Ni. It is also seen that the solubility of W in the γ phase increases with increasing Ni content.

The partition coefficient $K_x^{\gamma'/\gamma}$ $(= C_x^{\gamma'}/C_x^{\gamma})$ of each element in (82.5–x)Co-xNi-10Al-7.5W at 900°C is listed in Table 2 and plotted in Fig. 3(a), where $C_x^{\gamma'}$ and C_x^{γ} are equilibrium compositions of element x in the γ' and γ phases. It is clear that Al preferentially concentrates in the γ' phase rather than in the γ phase and that the partition coefficient of Al increases with increasing Ni content. The partition coefficient of W, which is high in the 10Ni alloy, decreases with increasing Ni content, reaching a region below $K_W^{\gamma'/\gamma} = 1.0$ at about 50% Ni, which means that W changes from a γ' former to a γ former by increase of Ni composition. The variation of partition coefficient of W in various alloys with different W content at 900°C is shown in Fig. 3(b). In the low W and Ni alloys, it is seen that W tends to concentrate in the γ' phase. This composition dependence of W is similar to the partition behavior of Mo in Ni-Al alloy.[16]

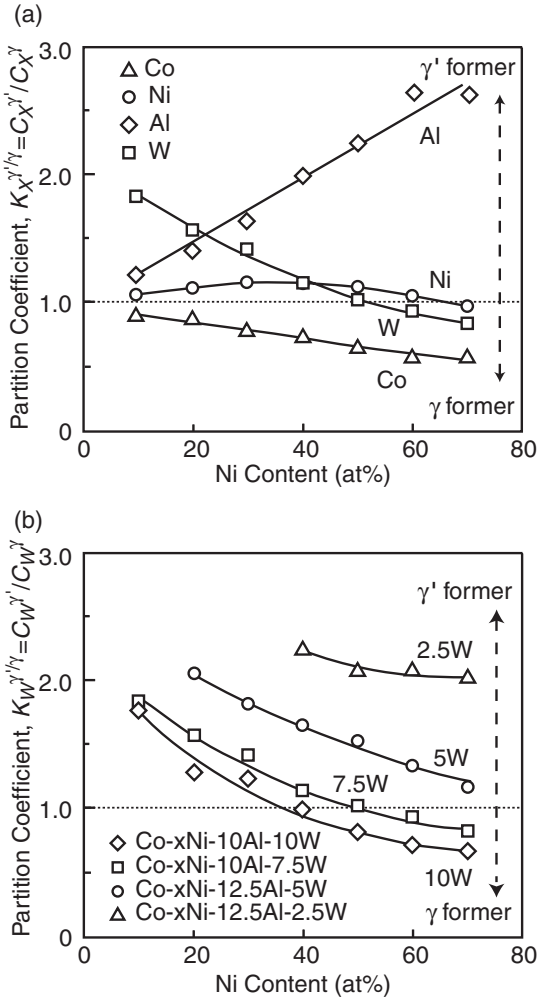

Fig. 3 Variation of (a) partition coefficient $K_x^{\gamma'/\gamma}$ $(= C_x^{\gamma'}/C_x^{\gamma})$ of each element in Co-xNi-10Al-7.5W at 900°C and (b) partition coefficient $K_W^{\gamma'/\gamma}$ of Co-Ni-Al-W alloys with various W contents.

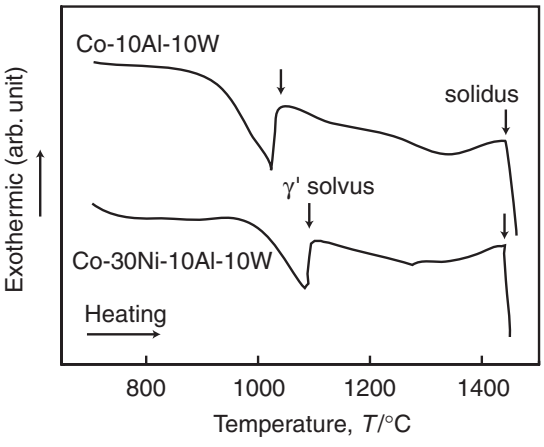

Fig. 4 DSC heating curves of Co-10Al-10W and Co-30Ni-10Al-10W alloys.

Figure 4 shows the typical DSC heating curves obtained from Co-30Ni-10Al-10W alloy after solution-treatment at 1300°C for 24 hours in comparison with Co-10Al-10W ternary alloy. There are endothermic peaks corresponding to γ' solvus and solidus temperatures described as $(\gamma + \gamma' \rightarrow \gamma)$ and $(\gamma \rightarrow \gamma + \text{liquid})$ reactions, respectively. Both the transition temperatures are defined as the end temperatures of the peaks during heating in this study and those of (80–x)Co-xNi-10Al-10W and (82.5–x)Co-xNi-10Al-7.5W alloys are plotted as a function of Ni content in Fig. 5(a). The γ' solvus temperature increases with increasing Ni content while the solidus temperature is hardly affected by the Ni content. It is also observed that the γ' solvus temperature increases with increasing W content from 7.5 at% to 10 at%.

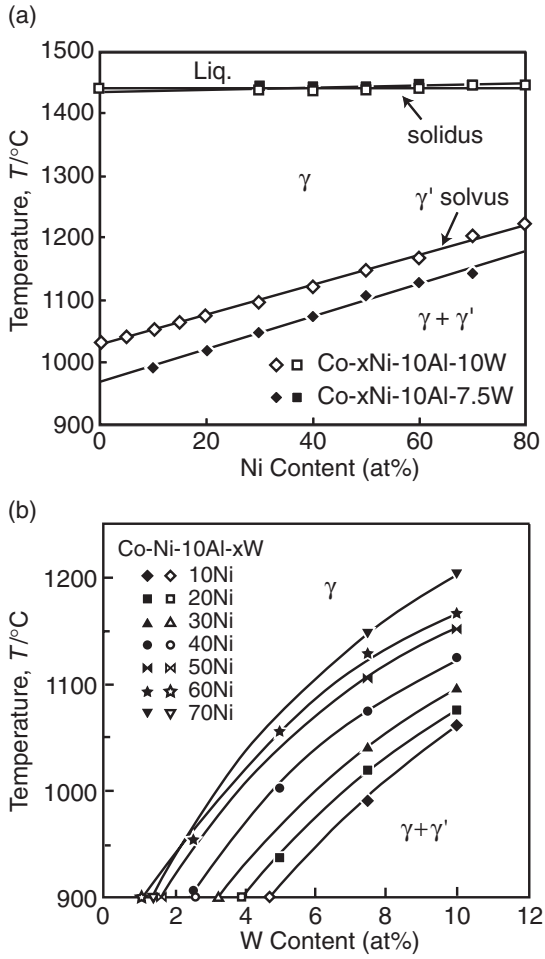

Fig. 5 (a) γ' solvus and solidus temperatures of Co-xNi-10Al-7.5W and Co-xNi-10Al-10W alloys. (b) Vertical section diagram of Co-Ni-10Al-W alloys with various Ni and W contents, showing the $\gamma/\gamma + \gamma'$ phase boundary, where the solid and open symbols indicate the data obtained by DSC and EPMA, respectively.

The vertical section diagram of Co-(10–70)Ni-10Al-W, which was obtained by the DSC measurements, and the phase boundary determined by EPMA in Table 1 and Fig. 2 is shown in Fig. 5(b), where the solid and open symbols indicate the data from DSC and EPMA, respectively. It is seen that the $\gamma/\gamma + \gamma'$ boundary monotonously increases with increasing Ni and W contents and that the substitution of Ni for Co is effective to increase the γ' solvus temperature, at least at the fixed Al content of 10 at%, except for the 70Ni alloys with low W content.

3.2 Microstructure and lattice parameter

Figure 6 shows FE-SEM images of the microstructure of (82.5–x)Co-xNi-10Al-7.5W alloys ($x = 10$, 40, 50 and 60)

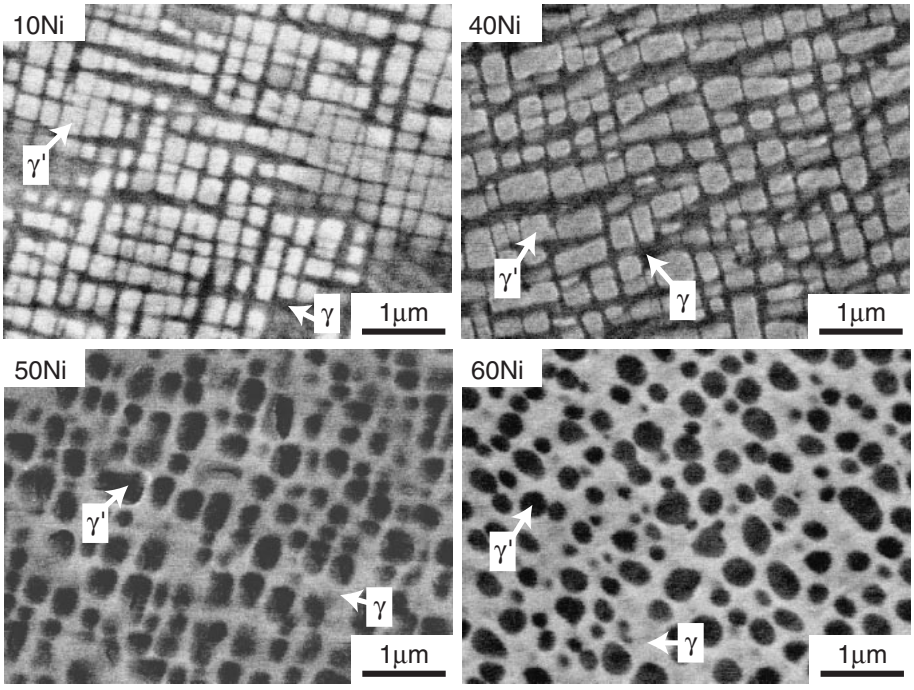

Fig. 6 SEM images of Co-10Ni-10Al-7.5W, Co-40Ni-10Al-7.5W, Co-50Ni-10Al-7.5W and Co-60Ni-10Al-7.5W annealed at 900°C for 168 hours.

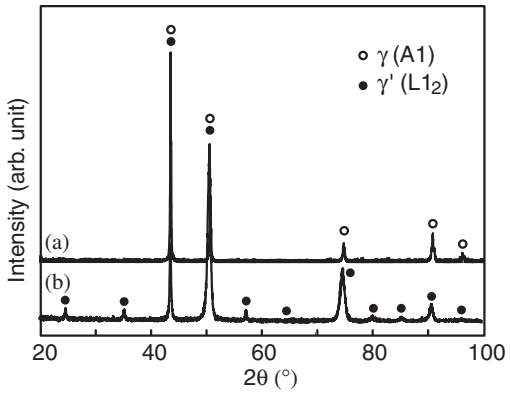

Fig. 7 XRD profile of (a) Co-27.7Ni-7.3Al-6.0W and (b) Co-32.6Ni-12.1Al-8.4W alloys cold-rolled at 50% reduction and annealed at 900°C for 168 hours. These alloy compositions correspond to the equilibrium compositions determined by EPMA for the Co-30Ni-10Al-7.5W alloy at 900°C.

annealed at 900°C for 168 hours. The 10Ni alloy shows cuboidal γ' precipitates 200–300 nm in size, and the morphology becomes spherical as Ni content increases. It is known that the morphology is affected by the lattice mismatch between the matrix and the precipitate; the γ' precipitates are formed as spheres at a 0%–0.2% mismatch, as cubes at about 0.5%–1.0% and as plates at above about 1.25% in Ni-based superalloys.[17] In order to clarify the origin of the morphological change dependent on the Ni content, XRD examination was carried out.

Since fundamental reflection lines of the γ and γ' phases obtained by the XRD technique overlap in Co-Ni-Al-W alloys due to the close lattice parameters, two alloys with equilibrium compositions in each (82.5–x)Co-xNi-10Al-7.5W two-phase alloy listed in Table 1 were prepared to determine the lattice parameters for the γ and γ' phases, the alloys being cold-rolled and subsequently annealed at 900°C for 168 hours. Although only a small amount of the γ phase was observed in some γ' phase specimens, the lattice parameter of each phase could be determined. Figure 7 shows XRD profiles of (a) Co-27.7Ni-7.3Al-6.0W and (b) Co-32.6Ni-12.1Al-8.4W alloys, corresponding to the equilibrium compositions of Co-30Ni-10Al-7.5W alloy at 900°C. Several ordering reflections from the $L1_2$ structure are seen in Co-32.6Ni-12.1Al-8.4W alloy having an almost γ' single-phase structure with only a small amount of the γ phase. The lattice parameter a_x for the γ and γ' phases determined by the above method are listed in Table 3 and plotted in Fig. 8 with the lattice mismatch δ between the γ and γ' phases which is defined as $\delta = 2(a_{\gamma'} - a_\gamma)/(a_{\gamma'} + a_\gamma)$. The lattice parameters of both the γ and γ' phases decrease with increasing Ni content, and the lattice mismatch also decreases from 0.4184% to 0.1958%.

Lattice parameters generally increase by the addition of solute atoms with larger atomic radius, and in fact, the lattice parameters of the γ-Co and the γ-Ni solid solutions increase by the addition of Al and W,[18,19] whose atomic radius is larger than that of Co and Ni. The lattice parameter change by the addition of Al and W in Co binary and Ni binary alloys is $+2.24 \times 10^{-4}$ nm/at% (Co-Al),[18] $+1.94 \times 10^{-4}$ nm/at% (Ni-Al),[19] $+3.52 \times 10^{-4}$ nm/at% (Co-W)[18] and $+4.48 \times 10^{-4}$ nm/at% (Ni-W),[19] which suggests that W more greatly affects the lattice parameter than Al. It has also been reported that the lattice parameter linearly decreases with increasing Ni content in Co-Ni alloy with the slope of -0.22×10^{-4} nm/at%,[20] obeying Vegard's law. Based on these previous data and the phase equilibria obtained in this study, it is considered that the decrease in the lattice parameters of the γ and γ' phases by the addition of Ni is

Table 3 Lattice parameter a_x of the γ and γ' phases, which was obtained in specimens having the equilibrium composition for Co-xNi-10Al-7.5W alloys at 900°C, and the lattice mismatch δ between the γ and γ' phases.

Co-xNi-10Al-7.5W	Specimen (Equilibrium Composition at γ Phase) (at%)			a_γ/nm	Specimen (Equilibrium Composition at γ' Phase) (at%)			$a_{\gamma'}$/nm	δ (%)
	Ni	Al	W		Ni	Al	W		
10Ni	9.7	8.7	5.4	0.3578	10.5	10.8	9.9	0.3593	0.4184
30Ni	27.7	7.3	6.0	0.3576	32.6	12.1	8.4	0.3587	0.3071
50Ni	46.5	6.0	6.9	0.3573	52.8	13.6	7.1	0.3582	0.2516
70Ni	70.3	5.6	7.6	0.3572	69.6	14.6	6.3	0.3579	0.1958

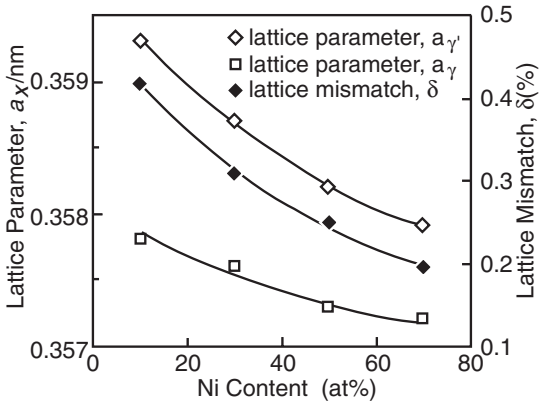

Fig. 8 Lattice parameters of the γ and γ' phases determined in the specimens with compositions equilibrated for Co-xNi-10Al-7.5W alloys at 900°C and the lattice mismatch. The compositions of the specimens are listed in Table 3.

predominantly influenced by the substitution of Ni for Co and that the decrease in the lattice mismatch between the γ and γ' phases is mainly attributable to the fact that W tends to distribute to the γ phase with increasing Ni content, in contrast to Al, as shown in Fig. 3(a).

Consequently, it is obvious that the variation of the morphology of the γ' phase in Fig. 6 is due to the change of the mismatch between the γ matrix and γ' precipitate as shown in Fig. 8.

4. Conclusions

Phase equilibria and microstructure on the γ' phase were examined in the Co-Ni-Al-W quaternary system. The results can be summarized as follows:

(1) The phase equilibria at 900°C were determined in the Co-(10–70)Ni-Al-W system, focusing on the γ and γ' phases. The γ' phase continuously exists from the Co side to the Ni side in the Co-Ni-Al-W system and the $\gamma' + \gamma$ two-phase is broadened with increasing Ni content.

(2) The partition of Al to the γ' phase increases while the W tends to be distributed to the γ phase with increasing Ni content.

(3) The γ' solvus temperature monotonously increases with increasing Ni content in the Co-xNi-10Al-7.5W and Co-xNi-10Al-10W alloys, although the solidus temperature is hardly affected by the Ni content.

(4) The lattice parameters of the γ and γ' phases in Co-(10–70)Ni-Al-W alloys decrease with increasing Ni content. The lattice mismatch between the γ and γ' phases also decreases with increasing Ni content and the range of the mismatch is approximately between 0.2 and 0.4.

(5) The morphology of the γ' precipitates in the γ matrix structure is cuboidal in low Ni alloys, while it shows spheres with increasing Ni content, particularly over 50 at%Ni, which is due to the decrease in the lattice mismatch originating from the partition change of Al and W.

Acknowledgment

This work was supported by a Grant-in-Aid for Scientific Research from the Japan Society for the Promotion of the Science. Support from CREST, Japan Science and Technology Agency is also acknowledged.

REFERENCES

1) P. Viatour, J. M. Drapier and D. Coutsouradis: Cobalt **3** (1973) 67–74.
2) J. M. Drapier, J. L. DE Brouwer and D. Coustsouradis: Cobalt **27** (1965) 59–72.
3) J. M. Drapier and D. Coustsouradis: Cobalt **39** (1968) 63–74.
4) J. M. Blaise, P. Viatour and J. M. Drapier: Cobalt **49** (1970) 192–195.
5) A. J. Bradley and G. C. Seager: J. Inst. Met. **64** (1939) 81–91.
6) O. S. Edwards: J. Inst. Met. **67** (1941) 67–77.
7) T. Omori, Y. Sutou, K. Oikawa, R. Kainuma and K. Ishida: Mat. Sci. Eng. A **438** (2006) 1045–1049.
8) J. Dutkiewicz and G. Kostorz: Acta Metall. Mater. **38** (1990) 2283–2286.
9) J. Dutkiewicz and G. Kostorz: Mater. Sci. Eng. A **132** (1991) 267–272.
10) J. Sato, T. Omori, K.Oikawa, I. Ohnuma, R. Kainuma and K. Ishida: Science **312** (2006) 90–91.
11) A. Suzuki, G. C. DeNolf and T. M. Pollock: Scr. Mater. **56** (2007) 385–388.
12) S. Miura, K. Ohkubo and T. Mohri: Mater. Trans. **48** (2007) 2403–2408.
13) A. Suzuki and T. M. Pollock: Acta Mater. **56** (2008) 1288–1297.
14) R. Kainuma, M. Ise, C.-C. Jia, H. Ohtani and K. Ishida: Intermetallics **4** (1996) S151–S158.
15) J. B. Nelson and D. P. Riley: Proc. Phys. Soc. **57** (1944) 160–177.
16) C. C. Jia, K. Ishida and T. Nishizawa: Metall. Mater. Trans. A **25A** (1994) 473–485.
17) E. W. Ross and C. T. Sims: *Superalloys II*, (A Wiley-Interscience Publication, New York, 1987) pp. 97–133.
18) T. Takayama, M. Y. Wey and T. Nishizawa: Trans. JIM **22** (1981) 315–325.
19) Y. Mishima, S. Ochiai and T. Suzuki: Acta Metall. **33** (1985) 1161–1169.
20) T. Nishizawa and K. Ishida: *Phase Diagrams of Binary Nickel Alloys*, (ASM International, Ohio, 1991) pp. 69–74.